

Dehydrogenation of Ammonia Borane Impacts Valence and Core Electrons: A Photoemission Spectroscopic Study

Delano P. Chong and Feng Wang*

Cite This: *ACS Omega* 2022, 7, 35924–35932

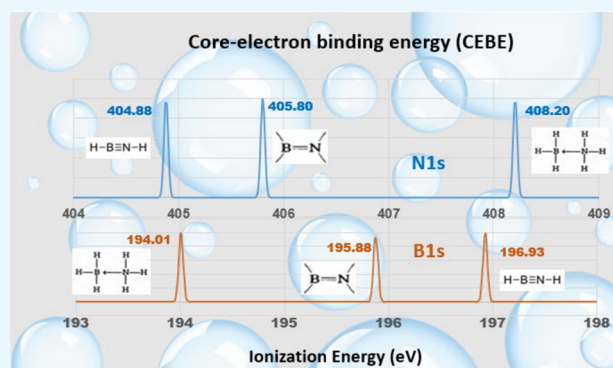
Read Online

ACCESS |

Metrics & More

Article Recommendations

ABSTRACT: Ammonia borane (H_3BNH_3) is a promising material for hydrogen storage and release. Dehydrogenation of ammonia borane produces small boron–nitrogen hydrides such as aminoborane (H_2BNH_2) and iminoborane (HBNH). The present study investigates ammonia borane and its two dehydrogenated products for the first time using calculated photoemission spectra of the valence and core electrons. It is found that a significant decrease in the dipole moment was observed associated with the dehydration from 5.397 D in H_3BNH_3 , to 1.942 D in H_2BNH_2 , and to 0.083 D in HBNH. Such reduction in the dipole moment impacts properties such as hydrogen bonding, dihydrogen bonding, and their spectra. Dehydrogenation of H_3BNH_3 impacts both the valence and core electronic structure of the boron–nitrogen hydrides. The calculated valence vertical ionization energy (VIE) spectra of the boron–nitrogen hydrides show that valence orbitals dominated by 2p-electrons of B and N atoms exhibit large changes, whereas orbitals dominated by s-electrons, such as $(3a_1, 4a_1, 5a_1/3\sigma, 4\sigma, 5\sigma)$ remain less affected. The first ionization energy slightly increases from 10.57 eV for H_3BNH_3 to 11.29 eV for both unsaturated H_2BNH_2 and HBNH. In core space, the oxidative dehydrogenation of H_3BNH_3 affects the core electron binding energy (CEBE) of borane and nitrogen oppositely. The B1s binding energies increase from 194.01 eV in H_3BNH_3 to 196.93 eV in HBNH, up by 2.92 eV, whereas the N1s binding energies decrease from 408.20 eV in H_3BNH_3 to 404.88 eV in HBNH, dropped by 3.32 eV.

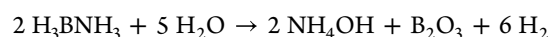


1. INTRODUCTION

Hydrogen (H_2) storage and controlled release from high content hydrogen compounds such as ammonia borane (AB, aminotrihydridoboron or borazane) is paramount to the hydrogen energy life cycle. AB (H_3BNH_3) has been considered as a promising solid hydrogen carrier as it is an excellent source of hydrogen (19.4 wt %) for fuel cell applications.¹ AB is a nontoxic, environmentally benign, and a stable material that can be safely transported without hydrogen loss, which dictates the success of any chemical for hydrogen storage.² AB dehydrogenation renders B–N oligomers and polymers as byproducts that are suitable starting materials for the synthesis of boron nitride (BN) ceramics.³ Although dehydrogenation of AB can be carried out under simple thermal conditions, insufficient kinetic control of the process leads to the formation of ill-defined B–N containing solids. This can be a serious drawback for the H_2 -depleted material recycling.¹

AB (H_3BNH_3) is the simplest amine boranes, yet its history has been anything but simple.⁴ First reported in 1955, AB is isoelectronic with ethane ($\text{H}_3\text{C}-\text{CH}_3$). It has exceptional properties for chemical hydrogen storage, and in recent years, it may have been dehydrogenated by multiple paths including

solvolysis (typically hydrolysis) and thermolysis (either in solution or the solid state).⁵ For example,



AB is stable under an inert atmosphere and at room temperature. For the destabilization of AB for thermolytic H_2 generation, there are still rooms for improvement.⁵ For example, AB is composed of three protic and three hydridic hydrogens that are able to react under heating to generate H_2 at temperatures from 100 °C and is able to release two equivalents of H_2 below 200 °C. An extensive overview has been given by Demirci⁵ covering 1955–2016 literature studies dedicated to ammonia borane's fundamentals and exceptional properties, including main achievements, limitations, and challenges for chemical hydrogen storage. As a result,

Received: July 22, 2022

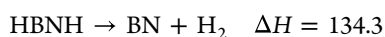
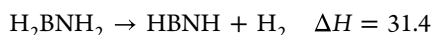
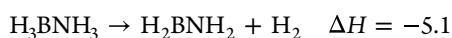
Accepted: August 24, 2022

Published: September 29, 2022

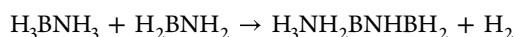
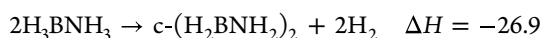


understanding of the electronic structures of AB and its dehydrogenated products such as geometries, stabilities, and ionization energies are very important for the study of the most economic hydrogen release mechanism. In addition, intermolecular interactions of AB such as hydrogen and dihydrogen bonds also play a significant role in the properties of AB during and before dehydrogenation.

The dehydrogenation (or oxidization) of AB produces unsaturated borane hydrides such as aminoborane (H_2BNH_2) and iminoborane (HBNH) with planar and linear configurations, respectively. They are essential for developing chemical methods of hydrogen release and regeneration of chemical hydrogen storage materials. The calculated energies for the sequential dehydrogenation of AB in the gas phase at 298 K are reported (in kcal/mol).⁶ For example,



There are other reactions to release hydrogen, such as,⁶



$$\Delta H = -11.5$$

Small boron–nitrogen hydrides are often polar analogues of hydrocarbons.⁷ AB ($\text{H}_3\text{B}-\text{NH}_3$) and unsaturated aminoborane ($\text{H}_2\text{B}=\text{NH}_2$) and iminoborane ($\text{HB}\equiv\text{NH}$) are isoelectronic hydrocarbon compounds of ethane (CH_3-CH_3), ethene ($\text{CH}_2=\text{CH}_2$), and ethyne ($\text{CH}\equiv\text{CH}$), respectively. The dehydrogenated (or oxidized) products of AB, however, has much different properties from its hydrocarbon analogues as the B–N bond is polar and contains protic and hydridic hydrogens.

A number of theoretical studies for AB and its dehydrogenated products (or small boron–nitrogen hydrides) has been performed.⁶ For example, average B–H and N–H bond dissociate energy (BDEs) for a range of main group compounds obtained from isodesmic reactions have been reported using MP4(SDTQ)/6-311++G(3df,2p) calculations.⁸ Kirwan and Roberts estimated the B–H and N–H BDEs for BH_3NH_3 with MP3/6-31G** calculations.⁹ Matus et al.¹⁰ calculated the standard heat of formation of small boron–nitrogen hydrides in the gas phase using high-accuracy ab initio electronic structure theory calculations of thermodynamic parameters at the coupled-cluster CCSD(T) level with energies extrapolated to the complete basis set (CBS) limit. Other properties, such as ionization energy of a molecule quantifies the energy required to remove an electron from the system. As such, it is a fundamental quantity in the context of redox chemistry, charge transfer, and molecular electronics,¹¹ which is also important for the understanding of kinetics and the mechanism of the processes releasing H_2 and regenerating the compounds in different molecular forms.^{6,10} However, to our knowledge, available ionization energy studies are only limited to the first ionization energies rather than complete valence and core spaces of the small boron–nitrogen hydrides.

The valence ionization energies of these boron–nitrogen hydrides are not available, nor their core electron binding energies (CEBEs). The first ionization energy (IE) of AB obtained by Yuan et al.¹² using mass spectroscopy (MS) was

given by 10.58 eV (vertical) and by 9.44 eV (adiabatic),¹² which agrees well with the calculated value of 10.61 eV using CCSD(T)/CBS for vertical IE¹³ and 9.29 eV,^{6,10} for adiabatic IE using different methods. No other valence IEs for aminoborane ($\text{H}_2\text{B}=\text{NH}_2$) is available except for the first. The first IE of the compound was measured using MS at 11.0 ± 0.1 eV¹⁴ and the same energy was calculated to be 10.62 eV using CCSD(T)/CBS.⁶ Similarly, no other valence IEs were available for iminoborane ($\text{HB}\equiv\text{NH}$), but the first IE of the compound was recently measured at 11.31 ± 0.02 eV using photoelectron–photoion coincidence spectroscopy (CRF-PEPICO),¹⁵ in agreement with an earlier calculation of 11.27 eV using the CCSD(T)/CBS method.⁶ To our knowledge, no CEBEs of the boron–nitrogen hydrides are available, neither in theory nor in experiment. The present study is to explore both complete valence and core ionization energies (i.e., photoemission spectra) of these boron–nitrogen hydrides (H_nBNH_n , $n = 1-3$), which are critical to establishing the most economic hydrogen release mechanism.

2. COMPUTATIONAL DETAILS

The ground electronic structures of three boron–nitrogen hydrides H_nBNH_n ($n = 1-3$) are studied in the gas phase. Geometry optimization of the stationary points was based on coupled-cluster theory [CCSD(T)] with the correlation-consistent polarized triple-zeta basis set, abbreviated as the CCSD(T)/cc-pVTZ level of calculation. Based on the optimized geometries of the small nitrogen hydrides, the complete valence vertical ionization energies (VIEs) are calculated in the gas phase using three different methods, including the $\Delta\text{PBE0}(\text{SAOP})/\text{et-pVQZ}$ method developed by Segala and Chong,¹⁶ the meta-Koopmans' theorem (mKT) and the outer valence Green's function (OVGF) method.¹⁷⁻¹⁹

The cc-pVTZ basis set is a standard one in the Gaussian program²⁰ and the et-pVQZ basis set is an even-tempered Slater-type basis set^{21,22} which is a standard one in the Amsterdam Density Functional (ADF) program.²³ The et-pVQZ functions are polarized valence quadruple zeta with even-tempered basis functions (similar to cc-pVQZ), which use even-tempered 1s, 2p, 3d, etc. functions without higher quantum number members such as 2s, 3s, ..., 3p, 4p, ... and hereby enable faster approximation of the integrals. Unlike the Gaussian type cc-pVnZ basis sets, the et-pVnZ basis sets use Slater-type orbitals (without contraction) which allows more flexible coverage of the core region. The et-pVQZ basis set in the present study was tested against a very large basis set of QZ4P.²⁴ This all-electron QZ4P basis set is triple zeta in the core and quadruple zeta in the valence region.²⁴ The even-tempered basis et-pVQZ is an adequate basis for the representation of Hartree–Fock atomic orbitals.²²

The $\Delta\text{PBE0}(\text{SAOP})/\text{et-pVQZ}$ method¹⁶ calculates energy difference with $E_{\text{xc}} = \text{PBE0}$ calculation with SAOP (statistical average of orbital potentials) densities.²⁵ The mKT calculations directly assume that the VIE is the negative of the orbital energies of the boron–nitrogen hydrides from SCF calculation of the density functional theory (DFT) where $V_{\text{xc}} = \text{SAOP}$.²⁵ The OVGF/et-pVQZ method performs electron propagator calculations for electron ionization or electron attachment processes where the frozen-orbital, single determinant picture of Koopmans' theorem is qualitatively valid.¹⁹ The calculated pole strength (PS) needs to be no smaller than 0.80 or the OVGF method is inapplicable as the one-electron approximation (molecular orbital picture) may break. A recent

benchmarking study²⁶ has compared the calculated valence ionization and core ionization spectra of indole and azaindoles in the gas phase against available experimental measurements. Excellent agreement has been achieved.²⁶

The CEBE calculations use the $\Delta(\text{PW86-PW91}/\text{et-pVQZ}) + C_{\text{rel}}$ method.²⁷ It takes the energy difference with Vxc of PW86²⁸ for exchange and PW91²⁹ for correlation and empirically determined relativistic effects (C_{rel}).²⁷ This method has been employed to accurately produce ionization potentials for a large number of compounds, including antioxidants,³⁰ radio sensitizers,³¹ dipeptides,³² other biomolecules,³³ and drugs,^{34–36} for synchrotron sourced X-ray photoelectron spectroscopic (XPS) measurements in the past decades. Errors of mKT tend to be about 0.4 eV for valence IPs and as large as 16 eV for CEBE of C1s.²⁶

All calculations were performed using the Gaussian 09 computational chemistry package²⁰ and ADF suites of programs.²³

3. RESULTS AND DISCUSSION

3.1. Properties of Small Boron–Nitrogen Hydrides (H_nBNH_n , $n = 1, 2$, and 3). The boron–nitrogen hydrides (H_nBNH_n , $n = 1–3$) are of fundamental interest. As a promising hydrogen carrier, AB (H_3BNH_3) can be heated to release hydrogen and polymers of aminoborane (H_2BNH_2) and monomeric iminoborane (HBNH) intermediates in the laser-induced preparation of nanodimensional BN.^{37,38} Both aminoborane ($\text{H}_2\text{B}=\text{NH}_2$) and iminoborane (HBNH) have only been synthesized in low temperature matrices and oligomerizes above -150 °C for aminoborane ($\text{H}_2\text{B}=\text{NH}_2$)³⁹ and below -233 °C (40 K) for iminoborane (HBNH).^{40–42} The calculated structural properties of the boron–nitrogen hydrides are given in Table 1. Among the

state electronic structures of the boron–nitrogen hydrides, i.e., iminoborane (HBNH), aminoborane (H_2BNH_2), and AB (H_3BNH_3) are linear with $C_{\infty v}$, planar C_{2v} , and a three-dimensional C_{3v} point group symmetry, respectively, as indicated in Table 1.

The agreement of the calculated B–N bond lengths of the boron–nitrogen hydrides is excellent with literature values, indicating that the present calculations are sufficiently accurate, and the method used is adequate. For example, the B–N bond lengths of HBNH, H_2BNH_2 , and H_3BNH_3 are 1.243, 1.394, and 1.655 Å, accordingly, which are in excellent agreement with literature values of 1.24, 1.39, and 1.66 Å, respectively. For comparison, the calculated C–C bond lengths of $\text{CH}\equiv\text{CH}$, $\text{CH}_2=\text{CH}_2$, and CH_3CH_3 using the same method⁴⁷ are 1.203, 1.334,⁴⁷ and 1.538 Å,⁴⁸ which are all shorter than the corresponding boron–nitrogen hydrides. The rotational constants (A, B, and C) of the boron–nitrogen hydrides also agree well with the available microwave measurement of H_2BNH_2 .⁴⁶ For example, the rotational constants of H_2BNH_2 are calculated to be 139,195, 27,433, and 22,917 MHz, respectively, which are quite close to the rotational constants of ethylene (C_2H_4) of 145,878, 30,019, and 24,835 MHz, respectively.⁴⁹ As a saturated boron–nitrogen-hydride, AB is in fact a complex of H_3B and NH_3 and the B–N single bond is formed by the donation of the lone electron pair from NH_3 (dative bond),⁴⁶ which is significantly different from the C–C bond in hydrocarbons. The complexation energy (E_c) of H_3BNH_3 with -25.97 kcal/mol agrees with such calculated energies summarized by Demirci.⁵ The complexation energies are calculated as the energy differences between the complex (e.g., H_3BNH_3) and the respective donor–acceptor moieties (H_3B and NH_3) in the gas phase. The B–N bonding of the unsaturated borane nitrogen hydrides, such as H_2BNH_2 and HBNH, is quite different from AB.

The boron–nitrogen hydrides may form hydrogen bonding, such as $\text{N}-\text{H}\cdots\text{B}$, where N–H is the (hydrogen) donor and B is the acceptor. The electron negativity of N, B, and H is 3.04, 2.04, and 2.20, respectively, and hydrogen has a higher electronegativity than boron, but a lower one compared to nitrogen. The more electronegative N atom withdraws electron density from the N–H bond, so that the hydrogen in N–H possesses a partial positive charge. The acceptor B atom stabilizes the positive charge, typically through a lone or nonbonding pair of electrons. As such, the hydrogens bonding to boron are slightly hydridic and to nitrogen are protonic. For example, the calculated Mulliken charge population of H_3BNH_3 is given by B ($-0.29e$), N ($-0.91e$), H_N ($0.45e$), and H_B ($-0.05e$).⁵⁰ As a result, an ionic attractive interaction may form between these B–Hs(δ^-) and N–Hs(δ^+) on neighboring AB molecules, forming a ‘dihydrogen’ bond of $\text{B}-\text{H}(\delta^-)\cdots(\delta^+)\text{H}-\text{N}$. As a result, these boron–nitrogen hydrides can form various dimers through dihydrogen bonding.⁵¹ The B–N bond of the AB complex is formed via B–p and N–p hybridization and is dative in nature. The electron deficiency of the B atom induces a charge transfer, which results in hydrogen bonding and dipole–dipole interactions among H_3BNH_3 complexes.⁵⁰ The large dipole moment of AB of 5.397 D in Table 1 confirms this dative property of H_3BNH_3 . This calculated dipole moment agrees well with the literature value of 5.56 D.⁵ The dipole moment of aminoborane H_2BNH_2 is 1.942 D in good agreement with 1.758 D.⁴⁵ The dipole moment of HBNH is very small, which is given by 0.083 D so that HBNH exhibits a repulsive nature of

Table 1. Selected Electronic Properties of Small Boron–Nitrogen Hydrides (H_3BNH_3 , H_2BNH_2 , and HBNH)^a

properties	HBNH	H_2BNH_2	H_3BNH_3
structure	$\text{H}-\text{B}\equiv\text{N}-\text{H}$	$\text{H}_2\text{B}=\text{N}-\text{H}$	$\text{H}_3\text{B}-\text{N}-\text{H}_3$
symmetry	$C_{\infty v}$	C_{2v}	C_{3v}
ΔE (E_h)	2.407475	1.174139	0*
$R_{\text{B-N}}$ (Å)	1.243(1.24) ^b	1.394(1.39) ^b	1.655(1.649) ^b
μ (D)	0.083	1.942 ^c	5.397 ^d
A (MHz)	-	139195 ^c	73821
B (MHz)	32781	27433 ^c	17713
C (MHz)	32781	22917 ^c	17713

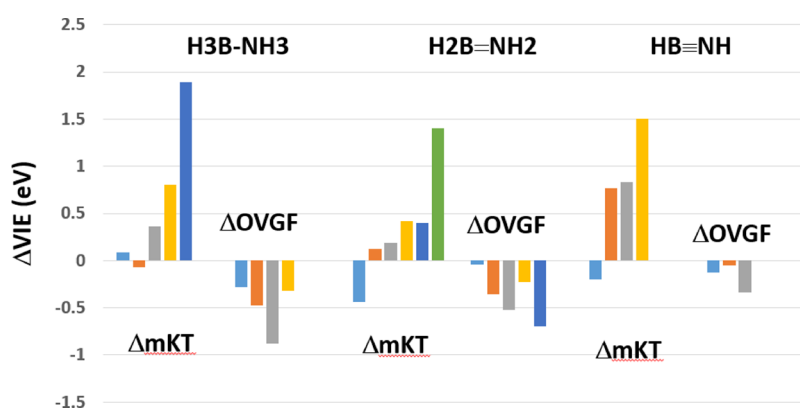
^aAll calculations are performed using the CCSD(T)/cc-pVTZ level of theory in this study. ^bRefer to the total energy of H_3BNH_3 of $-83.063511 E_h$. ^cThe results in parenthesis are from refs 5, 10. The B–N bond of H_3BNH_3 is given by 1.649 Å.⁴⁴ ^dCalculated dipole moment of H_2BNH_2 in the literature is 1.758 D.⁴⁵ ^eThe observed value of the gaseous state molecule of AB (H_3BNH_3) is 5.56 D.⁵ ^fAn earlier microwave measurement (1987) of the rotational constants was given by 138218.0, 27487.74, and 22878.52 MHz.⁴⁶

boron–nitrogen hydrides, aminoborane (H_2BNH_2) and monomeric iminoborane (HBNH) are unsaturated but AB (H_3BNH_3) is saturated with two isomers of eclipsed and staggered configurations. The difference between the eclipsed and the more stable staggered configuration of AB is very small (~ 2 kcal/mol)⁴³ under standard conditions, whereas in ethane (CH_3-CH_3), this energy difference is nearly five times larger at ~ 10 kcal/mol. As a result, the present study only considered eclipsed AB due to the high symmetry. The optimized ground-

Table 2. Comparison of Valence VIE of Ground Electronic States of Imonoborane (HBNH), Aminoborane (H₂BNH₂), and AB (H₃BNH₃) Using Different Methods (eV)^a

MO	H ₃ BNH ₃ (C _{3v})			MO	H ₂ BNH ₂ (C _{2v})			MO	HBNH(C _{∞v})		
	(3a ₁) ² (1e ₁) ⁴ (4a ₁) ² (5a ₁) ² (2e ₁) ⁴	ΔPBE0	mKT ^e		OvGF ^f	(3a ₁) ² (4a ₁) ² (1b ₂) ² (5a ₁) ² (2b ₂) ² (1b ₁) ²	ΔPBE0		mKT ^e	OvGF ^f	(3σ) ² (4σ) ² (5σ) ² (1π) ⁴
2e ₁ ^b	10.57	10.48	10.85	1b ₁ ^c	11.29	11.73	11.33	1π ^d	11.29	11.49	11.42
5a ₁	12.58	12.65	13.06	2b ₂	11.87	11.75	12.23	5σ	15.82	15.05	15.87
4a ₁	16.95	16.59	17.83	5a ₁	13.84	13.65	14.36	4σ	18.42	17.59	18.76
1e ₁	18.56	17.76	18.88	1b ₂	17.39	16.97	17.62	3σ	26.21	24.71	-
3a ₁	29.88	27.99		4a ₁	17.52	17.12	18.22				
				3a ₁	27.48	26.08					

^aHere, ΔPBE0 is the short for ΔPBE0(SAOP)/et-pVQZ. ^bExperiment (MS) VIE for 10.58 eV and adiabatic ionization energy (AIE) for 9.44 eV,¹² which agree well with a recent AIE of 9.26 ± 0.03 eV and VIE of 10.00 ± 0.03 eV, using photoelectron–photoion coincidence (PEPICO) spectroscopy.⁵² Theory with CCSD(T)/CBS, 9.29 eV.⁶ 896.4 kJ/mol (9.29 eV)¹⁰ and 997.7 kJ/mol (10.61 eV).¹³ ^cExperiment (MS) 11.0 ± 0.1 eV.¹⁴ Theory with CCSD(T)/CBS, 10.62 eV.⁶ ^dExperiment (CRF-PEPICO) 11.31 ± 0.02 eV.¹⁵ Theory with CCSD(T)/CBS, 11.27 eV.⁶ ^emKT, SAOP/et-pVQZ//CCSD(T)/cc-pVTZ. ^fOvGF/cc-pVQZ, where the spectroscopic PS is greater than 0.85.¹⁹

**Figure 1.** Comparison of deviation of the VIEs calculated using mKT and OVGF methods from the ΔPBE0 method.

intermolecular interaction. As a result, HBNH unlikely forms dimers.⁵¹

3.2. Ionization Energies and Photoemission Spectra of H_nBNH_n (n = 1, 2, and 3). Accurately determined properties such as IEs are crucial to establish the thermochemistry of the various steps in the H₂ release and recovery.¹⁵ The recently available experimental measurement from combustion reactions followed by photoelectron–photoion coincidence spectroscopy (CRF-PEPICO) using synchrotron radiation¹⁵ reported that the first IE of iminoborane (HBNH) is 11.31 ± 0.02 eV, which is in excellent agreement with 11.29 eV in the present study and 11.29 eV using the CCSD(T)/CBS⁶ for the same compound. The agreement indicates that the ionization process is a fast process, the ionized hole states (the cations) do not have time to relax so that the VIE model is appropriate. Table 2 reports the valence electron configurations and the complete valence VIEs of the boron–nitrogen hydrides. As the valence VIEs for the boron nitrogen hydrides did not exist before the present study, Table 2 compares the calculated VIEs using three different methods. In this table, the valence ground electronic configurations of the linear (C_{∞v}) iminoborane (HBNH), the planer (C_{2v}) aminoborane (H₂BNH₂), and the AB complex (C_{3v}) are also given. Iminoborane (HBNH) with 10 valence electrons occupies five doubly occupied molecular orbitals. The lowest occupied molecular orbital (HOMO) is a doubly degenerate 1π orbital and its VIE is 11.29 eV. It agrees well with 11.31 ± 0.02 eV measured using CRF-PEPICO.¹⁵ The VIEs of other

valence orbitals of this HBNH compound are well separated and spreading up to 26 eV.

The VIE energy differences between ΔPBE0 and mKT (Δ1) and OVGF (Δ2) of the boron–nitrogen hydrides are small in the outermost valence space but increase in the inner valence space due to stronger effects such as orbital relaxation. Figure 1 compares the ΔVIEs using three different methods. It is a known fact that the mKT method can be the least accurate method as it provides large error bars for the inner valence shell VIEs, whereas the OVGF method is able to provide quite accurate VIEs but the method does not apply to inner valence electron ionization. For the complete valence VIEs of the boron–nitrogen hydrides, the ΔPBE0 method can be the one which is sufficiently accurate and at the same time provides complete valence VIEs. As a result, the following discussion is based on the VIEs obtained using the ΔPBE0 method.

Addition of two hydrogen atoms to HBNH forms the planer aminoborane (H₂BNH₂) with a C_{2v} symmetry. A total of 12 valence electrons occupy six orbitals without energy degeneracy in the valence space. The VIE of the HOMO (1b₁) is given by 11.29 eV, HOMO-1 (2b₂) is 11.87 eV, HOMO-3 (1b₂) is 17.39 eV, and HOMO-4 (4a₁) is 17.52 eV, which are more closely located compared to the VIEs of HBNH. AB (H₃BNH₃) has 14 valence electrons which occupy seven orbitals with two pairs of doubly degenerate orbitals. The VIEs of the doubly degenerate HOMO (2e₁) is 10.57 eV and HOMO-3 (1e₁) is 18.56 eV. The other three occupied orbitals of AB spread up to 29.88 eV. It is noted that HBNH is subject to the Renner–Teller effect and H₃BNH₃ to a Jahn–Teller

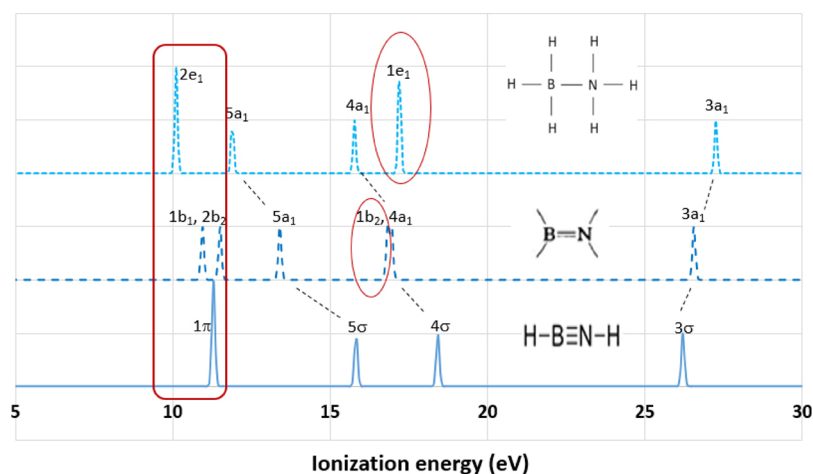


Figure 2. Valence VIEs of borane compounds (using the Δ PBE0 method). The ionization energies (degeneracy is considered) in Table 2 are convoluted using Gaussian broadening with full width at half maximum (FWHM) at 0.05 eV for photoelectron spectroscopic resolution.

effect. However, in their most recent experimental study, Schleier et al.¹⁵ indicated that the Renner–Teller splitting in the $X^{+2}\Pi'$ state of HBNH gives rise to two sets of vibrational progressions, separated by 70 meV, which is $\sim 0.62\%$ of the VIEs. As a result, the present study does not consider such effects.

It is noted that the VIE and AIE of ammonia borane (H_3BNH_3) can differ by as much as approximately ~ 1 eV,¹² as the structures of the cation and neutral AB can be quite different. This is confirmed by a measurement using photoelectron–photoion coincidence (PEPICO) spectroscopy of and AIE of 9.26 ± 0.03 eV and an VIE of 10.00 ± 0.03 eV.⁵² The present calculated VIE of AB at 10.57 eV agrees well with the measurements which are between the two experimental measurements of 10.58 eV¹² and 10.00 eV.⁵² In addition, our recent joint XPS experimental and theory study of hydroxybenzoic acids revealed that the vibrational impact is small for fast ionization processes⁵³ so that in the present study, only the first-order VIEs are considered. In addition, the fact that only the first IE available without any higher valence IEs of the boron–nitrogen hydrides also makes such high level calculations less useful. As a result, the present study calculates valence VIE for the boron–nitrogen hydrides.

Figure 2 reports the simulated valence ionization energy spectra of the boron–nitrogen hydrides based on the VIEs of the Δ PBE0 method in Table 2. The ionization spectra in this figure share certain similarities. Particularly between the spectra of AB (H_3BNH_3) and iminoborane (HBNH). When AB (H_3BNH_3) loses four Hs and becomes iminoborane (HBNH), it is equivalent to the removal of the doubly degenerate $1e_1$ orbital of AB (circled in the spectrum in Figure 2). Due to the molecule symmetry changes, the symmetric a_1 -orbitals become σ -orbitals and the doubly degenerate $2e_1$ -orbital (HOMO of AB) becomes a doubly degenerate 1π -orbital (HOMO) in HBNH. In the ionization spectrum of H_2BNH_2 (the middle spectrum in Figure 2) the orbitals are not degenerate. In this case, the doubly degenerate HOMO ($2e_1$) of AB (H_3BNH_3) splits into $1b_1$ and $2b_2$ orbitals in H_2BNH_2 for the C_{2v} symmetry, and the other doubly degenerate orbital $1e_1$ in AB becomes the $1b_2$ orbital in H_2BNH_2 due to the loss of two Hs. The VIE of $1b_2$ (17.39 eV) and VIE of $4a_1$ (17.52 eV) are closely located accidentally but with different symmetry. Finally, the orbitals such as (e_1 , b_1 and

b_2 and π) in the boron–nitrogen hydrides (highlighted in red) dominate the dehydrogenation of AB (H_3BNH_3) and its dehydrogenated products H_2BNH_2 and HBNH. These orbitals (e_1 , b_1 and b_2 and π) in the compounds are contributions of 2p electrons of B and N and are responsible for the unsaturated B–N bonding. The s-electron dominated symmetric orbitals such as ($3a_1, 4a_1, 5a_1/3\sigma, 4\sigma, 5\sigma$) exhibit minimal changes except for energy shifts.

In Figure 3, the ionization spectra of the isoelectronic hydrocarbons, ethane (C_2H_6), ethylene (C_2H_4), and acetylene (C_2H_2) are compared with the simulated ionization spectra of the boron nitrogen hydrides. The VIEs are taken from experimental measurements^{54,55} of the three hydrocarbons. The ionization spectrum (Figure 3c) of the linear acetylene (C_2H_2) shows similarities to the spectrum of HBNH, as they both have the same electron configurations of $(3\sigma)^2(4\sigma)^2(5\sigma)^2(1\pi)^4$, while the ionization energies of HBNH shift without changing the patterns but spanning in a larger energy region of (11.29, 26.21 eV). The outer valence electrons of HBNH on the orbitals of (4σ), (5σ), and (1π) are easier to ionize as they have smaller VIEs than the electrons in acetylene but the inner valence electron on the orbital (3σ) shifts to higher energy and therefore more difficult to ionize.

The ionization spectra of the planar H_2BNH_2 and C_2H_4 in Figure 3b perhaps is the most different spectra among the three isoelectronic compound pairs, although they have the same number of occupied orbitals. The electron configurations are different and the VIE patterns also different. The ground electronic state configuration of H_2BNH_2 is $\text{KK}-(3a_1)^2(4a_1)^2(1b_2)^2(5a_1)^2(2b_2)^2(1b_1)^2$ and the ethylene electronic configuration is given by $\text{KK}-(2a_g)^2(1b_{1u})^2(1b_{3u})^2(3a_g)^2(2b_{2g})^2(1b_{2u})^2$, as H_2BNH_2 and C_2H_4 belongs to different point group symmetries. The most apparent differences between the two spectra are that energies of the states with b-symmetries ($1b_{1u}$) and ($1b_{3u}$), as well as ($2b_{2g}$) and ($1b_{2u}$) in C_2H_4 , become closely located in H_2BNH_2 . It is interesting that the spectra of AB H_3BNH_3 and ethane CH_3CH_3 exhibit similarities except that the energies of the doubly degenerate $1e_u$ state and the $2a_{2u}$ state in ethane ($1e_u$, $2a_{2u}$) exchanged in H_3BNH_3 as ($4a_1$, $1e_1$). The common characters are shared among the boron nitrogen hydrides with respect to their isoelectronic hydrocarbons, such as (1) the first ionization energies of the boron nitrogen hydrides are smaller

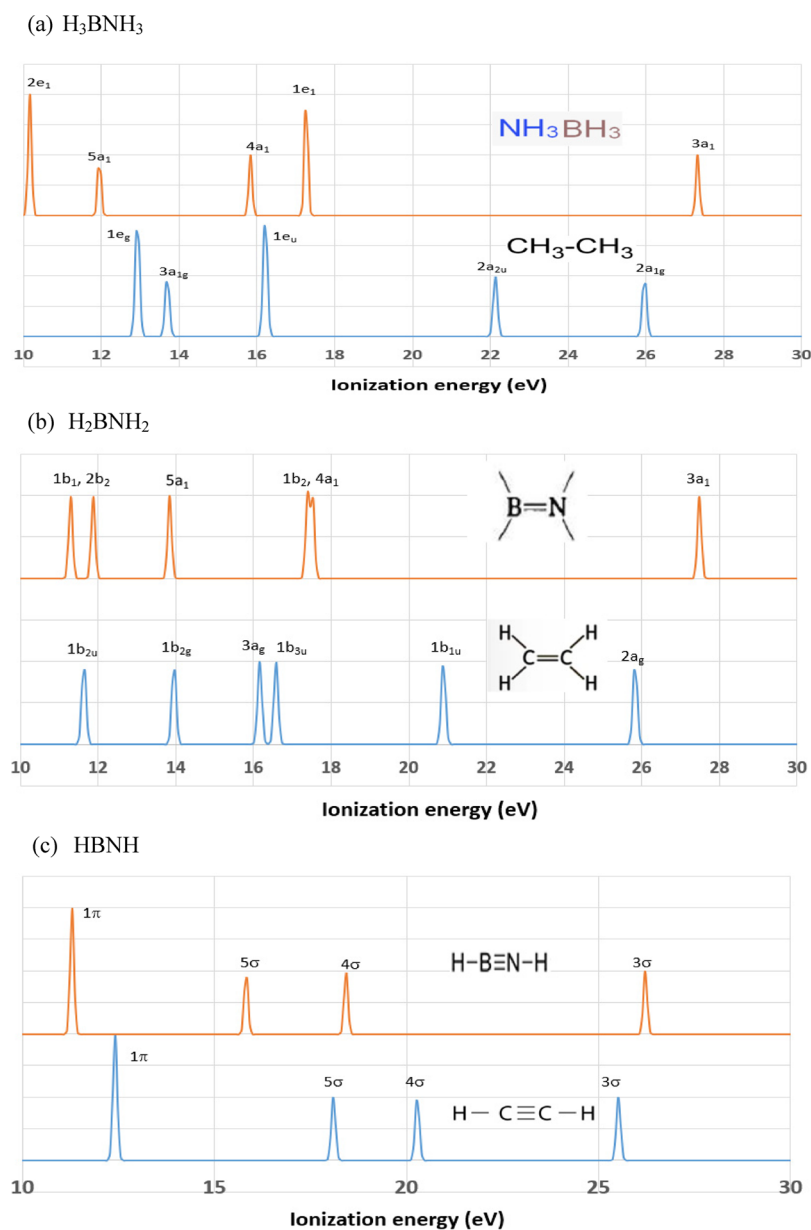


Figure 3. Comparison of the valence VIEs of borane nitrogen hydrides with their isoelectronic hydrocarbons. (a) VIE of H_3BNH_3 ; (b) VIE of H_2BNH_2 ; and (c) HBNH . The ionization energies (degeneracy is considered) of the hydrocarbons are taken from Bieri and Asbrink⁵⁴ convoluted using Gaussian broadening with FWHM at 0.05 eV for photoelectron spectroscopic resolution.

than their hydrocarbon counterparts, which means that the borane derivatives are easier to be ionized (oxidized), and (2) the valence ionization spectra of the boron nitrogen hydrides span a broader energy region than the hydrocarbons, suggesting that the inner valence electrons are more difficult to ionize.

We further calculated the CEBEs for B1s and N1s of the boron–nitrogen hydrides. There is only a single B1s experimental energy of 193.73 eV for AB (H_3BNH_3) available⁵⁶ which compares very well with the calculated B1s energy of 194.01 eV for the same molecule. Figure 4 compares the calculated CEBE of B1s and N1s of the three boron–nitrogen hydrides. As can be seen in the spectra, the CEBE of the B1s increases from 194.01 eV in H_3BNH_3 , to 195.88 eV in unsaturated H_2BNH_2 , and to 196.93 eV in HBNH with dehydrogenation. That is, B1s 194.01 eV (H_3BNH_3) < B1s 195.88 eV (H_2BNH_2) < B1s 196.93 eV (HBNH). Dehydro-

genation of the boron–nitrogen hydrides makes it more difficult to oxidize the boron core electrons. The CEBE of the N1s changes in an opposite trend, however. That is, the N1s binding energy decreases from 408.20 eV in H_3BNH_3 , to 405.80 eV in H_2BNH_2 , and to 404.88 eV in HBNH during dehydrogenation. That is, N1s 408.20 eV (H_3BNH_3) > N1s 405.80 eV (H_2BNH_2) > N1s 404.88 eV (HBNH). The N1s binding energies of the three boron–nitrogen hydrides are very similar to the N1s of C–N in nicotinamide (405–406 eV)⁵⁵ but lower than the experimental CEBE of $\text{N}\equiv\text{N}$ in the gas phase, which is given by 410.4 eV.⁵⁷ As a result, loss of hydrogens in the boron–nitrogen hydrides will make it less difficult to oxidize their nitrogen core electrons.

Positions of core electron ionization energies can be related to ionicity (i.e., the partial charges on various atoms), and the valence band density of states directly probes the electrons which are involved in bonding. CEBEs of the three boron–

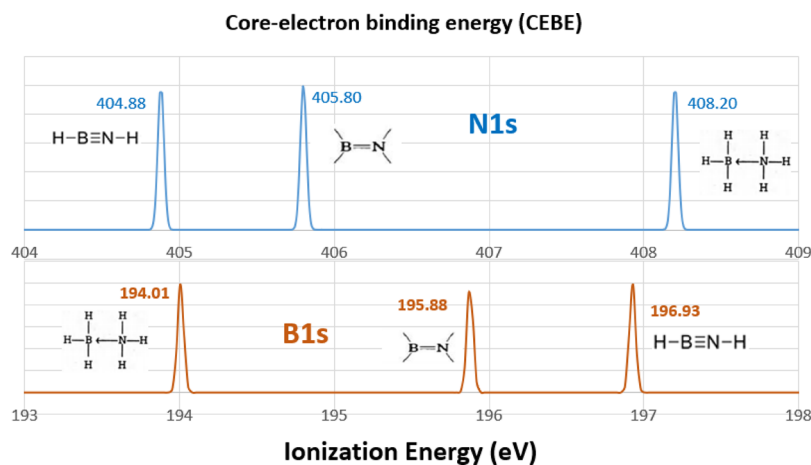


Figure 4. CEBEs of borane compounds. Orange for B1s energies and blue for N1s energies (eV).

nitrogen hydrides provide an opportunity to determine their correlations and more information about the nature of boron bonding. The available measured B1s energies for diborane (B_2H_6), $H_2BN(CH_2CH_3)_2$, $H_3BN(CH_2CH_3)_3$ are given by 196.5, 194.3, and 193.2 eV, respectively, and for H_3BNH_3 is 193.73 eV.⁵⁶ In the same measurement, the N1s energies of $H_2BN(CH_2CH_3)_2$ and $H_3BN(CH_2CH_3)_3$ are given as 404.7 and 406.2 eV, respectively, and for H_3BNH_3 is 408.41 eV,⁵⁶ which agree well with the present results. The information indicates that the results of the present study are reliable and informative for further measurements.

4. CONCLUSIONS

Complete valence VIEs and core electron ionization energies (CEBE) of AB (H_3BNH_3) and its dehydrogenated products aminoborane (H_2BNH_2) and iminoborane (HBNH) are calculated using an accurate quantum mechanical method for the first time. The obtained valence VIEs agree well with the available first IE measurements and other calculations. The CEBE of AB (H_3BNH_3) has excellent agreement with the B1s and N1s measurements. The valence VIE spectra of the three boron–nitrogen hydrides are closely related, depending on the number of hydrogen atoms, the B–N bond nature, and the symmetry of the compounds. We also compare the VIEs of the boron nitrogen hydrides with their isoelectronic hydrocarbon analogues of acetylene, ethylene, and ethane, similarities and differences are discussed. The boron nitrogen hydrides are found more oxidizable (ionizable) due to their smaller first ionization energies. Dehydrogenation of H_3BNH_3 to form H_2BNH_2 and to further form HBNH impacts both valence and core electronic space of the boron nitrogen hydrides. In particular, the valence p-electrons of B and N dominate their molecular chemical bonding at dehydrogenation, whereas the symmetric valence orbitals such as $(3a_14a_15a_1/3\sigma4\sigma5\sigma)$ remain less changed though with energy shift. The impact of dehydrogenation processes of the boron nitrogen hydrides is deep into the core electron region: the CEBE shift is opposite in B1s ionization energies and N1s ionization energies. The B1s energy of AB has the lowest CEBE energy of 194.01 eV whereas its N1s energy of the same molecule exhibits the highest CEBE of 408.20 eV among the three boron–nitrogen hydrides. When two pairs of H_2 are released from AB, the unsaturated HBNH compound exhibits the largest B1s energy of 196.93 eV with the lowest N1s energy of 404.88 eV. The

B1s CEBE increases by 2.92 eV and N1s CEBE reduces by 3.32 eV from H_3BNH_3 to HBNH.

The present study investigates the ionization processes in the valence and the core of the boron nitrogen hydrides. To further study the electronic structure and their behavior of these compounds may require information of other properties such as excitations of both valence and core electrons. As such, recent synchrotron sourced X-ray techniques including near-edge X-ray absorption fine structure (NEXAFS) enables an unambiguous identification of fingerprints for elements in molecules and core excitation spectra.⁵⁵ It will be interesting to use new measured NEXAFS of the boron–nitrogen hydrides in the near future to benchmark the existing extended second-order algebraic–diagrammatic construction approximation scheme for polarization propagator $ADC(2)x^{58,59}$ against the recently developed coupled-cluster (CC) theory obtained from a new time-dependent formalism based (EOM-CCSDT) and quadruples (EOM-CCSDTQ)^{60,61} for core excitation spectra.

AUTHOR INFORMATION

Corresponding Author

Feng Wang – Department of Chemistry and Biotechnology, School of Science, Computing and Engineering Technologies, Swinburne University of Technology, Melbourne, Victoria 3122, Australia; orcid.org/0000-0002-6584-0516; Email: fwang@swin.edu.au

Author

Delano P. Chong – Department of Chemistry, University of British Columbia, Vancouver, British Columbia V6T 1Z1, Canada

Complete contact information is available at:

<https://pubs.acs.org/10.1021/acsomega.2c04632>

Notes

The authors declare no competing financial interest.

ACKNOWLEDGMENTS

No external funding to acknowledge for this project.

REFERENCES

- (1) Ortega-Lepe, I.; Rossin, A.; Sánchez, P.; Santos, L. L.; Rendón, N.; Álvarez, E.; López-Serrano, J.; Suárez, A. Ammonia–Borane Dehydrogenation Catalyzed by Dual-Mode Proton-Responsive Ir-CNNH Complexes. *Inorg. Chem.* **2021**, *60*, 18490–18502.

- (2) Ramachandran, P. V.; Gagare, P. D. Preparation of Ammonia Borane in High Yield and Purity, Methanolysis, and Regeneration. *Inorg. Chem.* **2007**, *46*, 7810–7817.
- (3) Staubitz, A.; Presa Soto, A.; Manners, I. Iridium-Catalyzed Dehydrocoupling of Primary Amine–Borane Adducts: A Route to High Molecular Weight Polyaminoboranes, Boron–Nitrogen Analogues of Polyolefins. *Angew. Chem., Int. Ed.* **2008**, *47*, 6212–6215.
- (4) Li, H.; Yang, Q.; Chen, X.; Shore, S. G. Ammonia borane, past as prolog. *J. Organomet. Chem.* **2014**, *751*, 60–66.
- (5) Demirci, U. B. Ammonia borane, a material with exceptional properties for chemical hydrogen storage. *Int. J. Hydrogen Energy* **2017**, *42*, 9978–10013.
- (6) Dixon, D. A.; Gutowski, M. Thermodynamic Properties of Molecular Borane Amines and the [BH₄][NH₄⁺] Salt for Chemical Hydrogen Storage Systems from ab Initio Electronic Structure Theory. *J. Phys. Chem. A* **2005**, *109*, 5129–5135.
- (7) Huang, Z.; Wang, S.; Dewhurst, R. D.; Ignat'ev, N. V.; Finze, M.; Braunschweig, H. Boron: Its Role in Energy-Related Processes and Applications. *Angew. Chem., Int. Ed.* **2020**, *59*, 8800–8816.
- (8) Sana, M.; Leroy, G.; Wilante, C. Enthalpies of formation and bond energies in lithium, beryllium, and boron derivatives. A theoretical attempt for data rationalization. *Organometallics* **1991**, *10*, 264–270.
- (9) Kirwan, J. N.; Roberts, B. P. Homolytic reactions of ligated boranes. Part 11. Electron spin resonance studies of radicals derived from primary amine–boranes. *J. Chem. Soc., Perkin Trans. 2* **1989**, *5*, 539–550.
- (10) Matus, M. H.; Grant, D. J.; Nguyen, M. T.; Dixon, D. A. Fundamental Thermochemical Properties of Ammonia Borane and Dehydrogenated Derivatives (BNH_n, n = 0–6). *J. Phys. Chem. C* **2009**, *113*, 16553–16560.
- (11) Ranasinghe, D. S.; Margraf, J. T.; Perera, A.; Bartlett, R. J. Vertical valence ionization potential benchmarks from equation-of-motion coupled cluster theory and QTP functionals. *J. Chem. Phys.* **2019**, *150*, No. 074108.
- (12) Yuan, B.; Shin, J.-W.; Bernstein, E. R. Dynamics and fragmentation of van der Waals and hydrogen bonded cluster cations: (NH₃)_n and (NH₃BH₃)_n ionized at 10.51 eV. *J. Chem. Phys.* **2016**, *144*, 144315.
- (13) Lloyd, D. R.; Lynaugh, N. Photoelectron studies of boron compounds. Part 3.—Complexes of borane with Lewis bases. *J. Chem. Soc., Faraday Trans. 2* **1972**, *68*, 947–958.
- (14) McGee, H. A., Jr.; Kwon, C. Cryochemical preparation of monomeric aminoborane. *Inorg. Chem.* **1970**, *9*, 2458–2461.
- (15) Schleier, D.; Schaffner, D.; Gerlach, M.; Hemberger, P.; Fischer, I. Threshold photoelectron spectroscopy of iminoborane, HBNH. *Phys. Chem. Chem. Phys.* **2022**, *24*, 20–24.
- (16) Segala, M.; Chong, D. P. An evaluation of exchange–correlation functionals for the calculations of the ionization energies for atoms and molecules. *J. Electron Spectrosc. Relat. Phenom.* **2009**, *171*, 18–23.
- (17) Cederbaum, L. One-body Green's function for atoms and molecules: theory and application. *J. Phys. B: At. Mol. Phys.* **1975**, *8*, 290.
- (18) von Niessen, W.; Schirmer, J.; Cederbaum, L. S. Computational methods for the one-particle green's function. *Comput. Phys. Rep.* **1984**, *1*, 57–125.
- (19) Zakrzewski, V.; Ortiz, J.; Nichols, J. A.; Heryadi, D.; Yeager, D. L.; Golab, J. T. Comparison of perturbative and multiconfigurational electron propagator methods. *Int. J. Quantum Chem.* **1996**, *60*, 29–36.
- (20) Frisch, M. J.; et al. *Gaussian 09, Revision E.01*; Gaussian, Inc.: Wallingford, CT, USA, 2013.
- (21) Raffanetti, R. C. Even-tempered atomic orbitals. II. Atomic SCF wavefunctions in terms of even-tempered exponential bases. *J. Chem. Phys.* **1973**, *59*, 5936–5949.
- (22) Chong, D. P.; Van Lenthe, E.; Van Gisbergen, S.; Baerends, E. J. Even-tempered slater-type orbitals revisited: From hydrogen to krypton. *J. Comput. Chem.* **2004**, *25*, 1030–1036.
- (23) Baerends, E. J.; et al. *ADF2014; SCM Theoretical Chemistry*; Vrije Universiteit: Amsterdam, The Netherlands, 2014.
- (24) Van Lenthe, E.; Baerends, E. J. Optimized Slater-type basis sets for the elements 1–118. *J. Comput. Chem.* **2003**, *24*, 1142–1156.
- (25) Gritsenko, O. V.; Schipper, P. R. T.; Baerends, E. J. Approximation of the exchange–correlation Kohn–Sham potential with a statistical average of different orbital model potentials. *Chem. Phys. Lett.* **1999**, *302*, 199–207.
- (26) Chong, D. P. Computational study of the electron spectra of vapor-phase indole and four azaindoles. *Molecules* **2021**, *26*, 1947.
- (27) Chong, D. P. Density-functional calculation of core-electron binding energies of glycine conformers. *Can. J. Chem.* **1996**, *74*, 1005–1007.
- (28) Perdew, J. P.; Yue, W. Accurate and simple density functional for the electronic exchange energy: Generalized gradient approximation. *Phys. Rev. B* **1986**, *33*, 8800–8802.
- (29) Perdew, J. P.; Chevary, J. A.; Vosko, S. H.; Jackson, K. A.; Pederson, M. R.; Singh, D. J.; Fiolhais, C. Atoms, molecules, solids, and surfaces: Applications of the generalized gradient approximation for exchange and correlation. *Phys. Rev. B: Condens. Matter* **1992**, *46*, 6671–6687.
- (30) Islam, S.; Ganesan, A.; Auchettl, R.; Plekan, O.; Acres, R. G.; Wang, F.; Prince, K. C. Electronic structure and intramolecular interactions in three methoxyphenol isomers. *J. Chem. Phys.* **2018**, *149*, 134312.
- (31) Feketeová, L.; Plekan, O.; Goonewardane, M.; Ahmed, M.; Albright, A. L.; White, J.; O'Hair, R. A. J.; Horsman, M. R.; Wang, F.; Prince, K. C. Photoelectron Spectra and Electronic Structures of the Radiosensitizer Nimorazole and Related Compounds. *J. Phys. Chem. A* **2015**, *119*, 9986–9995.
- (32) Arachchilage, A. P. W.; Wang, F.; Feyer, V.; Plekan, O.; Prince, K. C. Correlation of electronic structures of three cyclic dipeptides with their photoemission spectra. *J. Chem. Phys.* **2010**, *133*, 174319.
- (33) Wickrama Arachchilage, A. P.; Wang, F.; Feyer, V.; Plekan, O.; Acres, R. G.; Prince, K. C. X-ray Photoemission Spectra and Electronic Structure of Coumarin and its Derivatives. *J. Phys. Chem. A* **2016**, *120*, 7080–7087.
- (34) Ahmed, M.; Wang, F.; Acres, R. G.; Prince, K. C. Structures of Cycloserine and 2-Oxazolidinone Probed by X-ray Photoelectron Spectroscopy: Theory and Experiment. *J. Phys. Chem. A* **2014**, *118*, 3645–3654.
- (35) Sa'adeh, H.; Backler, F.; Wang, F.; Piccirillo, S.; Ciavardini, A.; Richter, R.; Coreno, M.; Prince, K. C. Experimental and Theoretical Soft X-ray Study of Nicotine and Related Compounds. *J. Phys. Chem. A* **2020**, *124*, 4025–4035.
- (36) Hill, A.; Sa'adeh, H.; Cameron, D.; Wang, F.; Trofimov, A. B.; Larionova, E. Y.; Richter, R.; Prince, K. C. A comprehensive core level study of phenol, benzoic acid and three isomers of hydroxybenzoic acid. *J. Chem. Phys. A* **2021**, *125*, 9877–9891.
- (37) Swarnakar, A. K.; Hering-Junghans, C.; Nagata, K.; Ferguson, M. J.; McDonald, R.; Tokitoh, N.; Rivard, E. Encapsulating Inorganic Acetylene, HBNH, Using Flanking Coordinative Interactions. *Angew. Chem., Int. Ed.* **2015**, *54*, 10666–10669.
- (38) Demirci, U. B. Ammonia Borane: An Extensively Studied, Though Not Yet Implemented, Hydrogen Carrier. *Energies* **2020**, *13*, 3071.
- (39) Pons, V.; Baker, R. T.; Szymczak, N. K.; Heldebrant, D. J.; Linehan, J. C.; Matus, M. H.; Grant, D. J.; Dixon, D. A. Coordination of aminoborane, NH₂BH₂, dictates selectivity and extent of H₂ release in metal-catalysed ammonia borane dehydrogenation. *Chem. Commun.* **2008**, *48*, 6597–6599.
- (40) Paetzold, P. Iminoboranes. In *Adv. Inorg. Chem.*; Emeléus, H. J., Sharpe, A. G., Eds.; Academic Press, 1987; Vol. 31, pp 123–170.
- (41) Sundaram, R.; Scheiner, S.; Roy, A. K.; Kar, T. B=N Bond Cleavage and BN Ring Expansion at the Surface of Boron Nitride Nanotubes by Iminoborane. *J. Phys. Chem. C* **2015**, *119*, 3253–3259.
- (42) Swarnakar, A. K.; Hering-Junghans, C.; Ferguson, M. J.; McDonald, R.; Rivard, E. Reactivity of a coordinated inorganic acetylene unit, HBNH, and the azidoborane cation [HB(N₃)]⁺. *Chem. Sci.* **2017**, *8*, 2337–2343.

- (43) Parafiniuk, M.; Mitoraj, M. P. On the origin of internal rotation in ammonia borane. *J. Mol. Model.* **2014**, *20*, 2272.
- (44) Mitoraj, M. P. Bonding in Ammonia Borane: An Analysis Based on the Natural Orbitals for Chemical Valence and the Extended Transition State Method (ETS-NOCV). *J. Phys. Chem. A* **2011**, *115*, 14708–14716.
- (45) Minyaev, R. M.; Wales, D. J.; Walsh, T. R. Gradient Line Reaction Paths for Hindered Internal Rotation in H₂BNH₂ and Inversion in PF₃. *J. Phys. Chem. A* **1997**, *101*, 1384–1392.
- (46) Sugie, M.; Takeo, H.; Matsumura, C. Microwave spectrum and molecular structure of aminoborane, BH₂NH₂. *J. Mol. Spectrosc.* **1987**, *123*, 286–292.
- (47) Helgaker, T.; Gauss, J.; Jørgensen, P.; Olsen, J. The prediction of molecular equilibrium structures by the standard electronic wave functions. *J. Chem. Phys.* **1997**, *106*, 6430–6440.
- (48) Wiberg, K. B. Basis set effects on calculated geometries: 6-311++G** vs. aug-cc-pVDZ. *J. Comput. Chem.* **2004**, *25*, 1342–1346.
- (49) Van Lerberghe, D.; Wright, I. J.; Duncan, J. L. High-resolution infrared spectrum and rotational constants of ethylene-H₄. *J. Mol. Spectrosc.* **1972**, *42*, 251–273.
- (50) Zhong, B.; Song, L.; Huang, X. X.; Xia, L.; Wen, G. First-principles investigation of ammonia borane for hydrogen storage. *Phys. Scr.* **2012**, *86*, No. 015606.
- (51) Kar, T.; Scheiner, S. Comparison between hydrogen and dihydrogen bonds among H₃BNH₃, H₂BNH₂, and NH₃. *J. Chem. Phys.* **2003**, *119*, 1473–1482.
- (52) Schleier, D.; Gerlach, M.; Pratim Mukhopadhyay, D.; Karaev, E.; Schaffner, D.; Hemberger, P.; Fischer, I. Ammonia Borane, NH₃BH₃: A Threshold Photoelectron–Photoion Coincidence Study of a Potential Hydrogen-Storage Material. *Chem. – Eur. J.* **2022**, *28*, No. e202201378.
- (53) Hill, A.; Sa’adeh, H.; Cameron, D.; Wang, F.; Trofimov, A. B.; Larionova, E. Y.; Richter, R.; Prince, K. C. Positional and Conformational Isomerism in Hydroxybenzoic Acid: A Core-Level Study and Comparison with Phenol and Benzoic Acid. *J. Phys. Chem. A* **2021**, *125*, 9877–9891.
- (54) Bieri, G.; Åsbrink, L. 30.4-nm He(II) photoelectron spectra of organic molecules: Part I. Hydrocarbons. *J. Electron Spectrosc. Relat. Phenom.* **1980**, *20*, 149–167.
- (55) Pitts, T. C.; Lathiotakis, N. N.; Gidopoulos, N. Generalized Kohn–Sham equations with accurate total energy and single-particle eigenvalue spectrum. *J. Chem. Phys.* **2021**, *155*, 224105.
- (56) Beach, D. B.; Jolly, W. L. Photoelectron spectroscopic study of the bonding in borane adducts. *Inorg. Chem.* **1985**, *24*, 567–570.
- (57) Shah, D.; Bahr, S.; Dietrich, P.; Meyer, M.; Thißen, A.; Linford, M. R. Nitrogen gas (N₂), by near-ambient pressure XPS. *Surf. Sci. Spectra* **2019**, *26*, No. 014023.
- (58) Schirmer, J. Beyond the random-phase approximation: A new approximation scheme for the polarization propagator. *Phys. Rev. A* **1982**, *26*, 2395–2416.
- (59) Trofimov, A. B.; Schirmer, J. An efficient polarization propagator approach to valence electron excitation spectra. *J. Phys. B: At., Mol. Opt. Phys.* **1995**, *28*, 2299–2324.
- (60) Park, Y. C.; Perera, A.; Bartlett, R. J. Equation of motion coupled-cluster for core excitation spectra: Two complementary approaches. *J. Chem. Phys.* **2019**, *151*, 164117.
- (61) Park, Y. C.; Perera, A.; Bartlett, R. J. Equation of motion coupled-cluster study of core excitation spectra II: Beyond the dipole approximation. *J. Chem. Phys.* **2021**, *155*, No. 094103.